

# Non-Rigid-Registration of Breast Dynamic Contrast-Enhanced MRI Data: Comparison and Evaluation of B-splines and Symmetric Diffeomorphic Normalization based Methods

Venkata Veerendranadh Chebrolu<sup>1</sup>, Dattesh D Shanbhag<sup>1</sup>, Aurelie Le Deley<sup>2</sup>, Sheshadri Thiruvankadam<sup>1</sup>, Uday Patil<sup>1,3</sup>, Patrice Hervo<sup>2</sup>, Sandeep N Gupta<sup>4</sup>, and Rakesh Mullick<sup>5</sup>

<sup>1</sup>Medical Image Analysis Lab, GE Global Research, Bangalore, Karnataka, India, <sup>2</sup>GE Healthcare, Buc, France, <sup>3</sup>Manipal Health Enterprises Pvt. Ltd., Bangalore, Karnataka, India, <sup>4</sup>Biomedical Image Processing Lab, GE Global Research, Niskayuna, NY, United States, <sup>5</sup>Diagnostics and Biomedical Technologies, GE Global Research, Bangalore, Karnataka, India

**Target Audience:** Physicists and radiologists interested in non-rigid motion correction in breast dynamic contrast-enhanced (DCE)-MRI.

**Purpose:** DCE-MRI is increasingly being used in diagnosis and screening of breast tumors. Careful study of intensity changes over time between the pre-contrast and post-contrast images is critical to tumor biometry. Rigid and non-rigid motion may be caused by factors such as voluntary patient motion, cardiac pulsation, and breathing during image acquisition. A reduction of motion effects is important for valid morphological or dynamical image analysis [1]. Previous work [1] evaluated the efficacy of b-splines [2] based approaches in correcting for motion in breast DCE MRI. In this work we compare and evaluate b-splines and symmetric diffeomorphic normalization [3, 4] based non-rigid registration (NRR) algorithms for their effectiveness in motion correction for breast DCE-MRI.

**Methods:** NRR in the breast DCE data was compared and evaluated for four different approaches. *Method 1:* 3D symmetric diffeomorphic normalization based NRR [3] between the 3D volumes (phases) of the DCE intensity data. *Method 2:* 3D symmetric diffeomorphic normalization based NRR [3] between different phases of the DCE intensity data with NRR localization using a mask which includes the breast region and excludes the cardiac region. *Method 3:* 3D b-splines [5] based registration between the Laplacian transforms of different phases of the DCE data. A mask including the breast and cardiac region was used for localizing the motion correction. Laplacian was used to reduce the effect of contrast changes on NRR between different phases. *Method 4:* 3D b-splines [5] based NRR between the Laplacian transforms of the different phases. Same mask as Method 1 was used. In all the four methods, mutual information was used as the similarity metric and last-phase of the 4D data was used as the “fixed” image volume and other phases were registered to the last-phase. A multi-resolution framework was used for all the four methods with processing at three different resolutions. The number of iterations at different resolutions is represented by  $M \times N \times P$  ( $M$  iterations at 4 times lower resolution,  $N$  iterations at 2 times lower resolution and  $P$  iterations at the original data resolution). A grid-spacing of 15mm×15mm×15mm was used as the final grid-spacing in physical units [5] for the b-splines based deformation in the multi-resolution framework.

$$E[u] = \int_{\Omega} (1-u)^2 (1-c_{bgr})^2 dx + \int_{\Omega} \frac{\alpha}{1+\beta(1-c_{bgr})^2} dx + \gamma \int_{\Omega} (1-u)^2 dx + \lambda \int_{\Omega} |\nabla u|^2 dx \quad \text{Eq. [1]}$$

**Mask Generation:** The masks for the body and heart were generated using the phase field method [6, 7]. A two-class phase field formulation, shown in Equation 1, was used to segment the body mask from the first-phase and heart mask from the last-phase of the DCE data. In Equation 1,  $I$  is the weighted sum of image intensity and image gradient for the phase volume.  $u$  represents the two class function ( $u=1$  for the region of interest and

$u=0$  for the background).  $c_{bgr}$  is the reference intensity for the background. The parameters  $\alpha, \beta, \gamma$  and  $\lambda$  that control the noise variance, smoothness and sensitivity were empirically chosen. **Evaluation of the Four Methods:** An experienced radiologist evaluated the NRR results of the four methods by comparing result from each method with those of the other methods and the corresponding original data. The NRR performance was rated based on whether the motion present in the original data was corrected and whether or not any new deformations originally not present in the data were introduced by the NRR procedure. The time performance of the methods was also compared. The NRR processing was performed on a system with 8 core Intel Xenon CPU X5550 @2.67Hz processors with 11.7 GiB RAM. **Imaging:** Eighteen breast cancer patients were scanned on 1.5T GE Signa HDxt and 3T Signa Excite systems (GE Healthcare, Waukesha, WI) using typical DCE MRI imaging protocols with matrix sizes of 256×256 or 512×512 (in-plane resolution of 0.98mm×0.98mm to 0.63mm×0.63mm) in either axial or sagittal orientations with slice thicknesses of 0.8 to 4mm. The total number of slices ranged from 62 to 232. The studies were approved by an IRB.

**Results and Discussion:** **NRR Time Performance:** Figure 1a shows the average processing time taken by Method 1 for NRR between two phases. The NRR processing time diffeomorphic normalization based approaches was directly proportional to number of voxels per phase. Hence, the usage of mask in Method 2 reduced the NRR processing time by 40% on average. In contrast, independent of the number of voxels per phase, the average time that b-splines based methods took for NRR between two

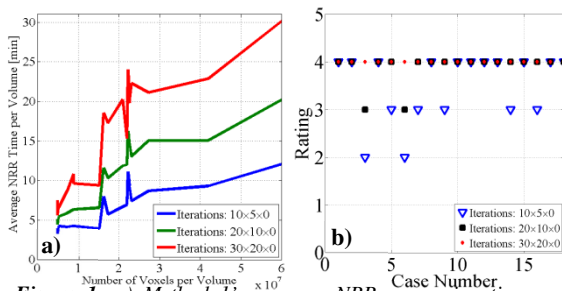


**Figure 1:** a) Method 1's average NRR processing time per volume at different number of voxels per volume. Results for three different iteration options in the multi-resolution framework are shown. b) Rating (0:worst to 4:best) by the experienced radiologist for the performance of Method 1 at different iteration options for the 18 cases.

was better than with inclusion of cardiac mask for b-splines based approaches. In contrast, the NRR accuracy of diffeomorphic approaches (Methods 1 and 2) did not change with or without use of mask in the region of interest defined by the mask. Figure 2 shows an example of the impact of NRR on the time courses in a ROI (shown in red) for a representative case. Qualitative visual assessment shows better NRR accuracy with Diffeomorphic normalization based methods. Work on quantitative measures for assessment of the efficacy of motion correction by NRR methods in DCE-MRI has been submitted separately. **Conclusions:** B-splines based NRR approaches provided consistent time performance, but introduced new deformations in some cases. The time performance of diffeomorphic normalization based NRR approaches changed from case to case depending on the number of voxels processed for NRR. However, better NRR accuracy was achieved and no new deformations were introduced. **References:** [1] Melbourne A et al, Phys Med Biol. 2011;56(24):7693-708. [2] Modat M et al, Comp Meth Prog Biom. 2010;98: 278-84. [3] Avants B et al, Penn Img Comp and Sci Lab. 2009. [4] Arno K et al, Neuroimage 2009;46(3):786-802. [5] Klein S et al, IEEE Trans on Med Img 2010;29(1):196-205. [6] Thiruvankadam et al. ICIP 2006. [7]. Samson et al. PAMI 2000; 22(5).

Case	Motion Corrected				New Deformations			
	Method No.				Method No.			
	1	2	3	4	1	2	3	4
A	Y	Y	Y	Y	N	N	N	N
B	Y	Y	Y	Y	N	N	N	N
C	Y	Y	Y	Y	N	N	Y	Y
D	Y	Y	Y	Y	N	N	N	N
E	Y	Y	Y	Y	N	N	N	N

**Table 1:** Evaluation of NRR accuracy of the four methods by an experienced radiologist in five cases (Y-Yes; N-No).

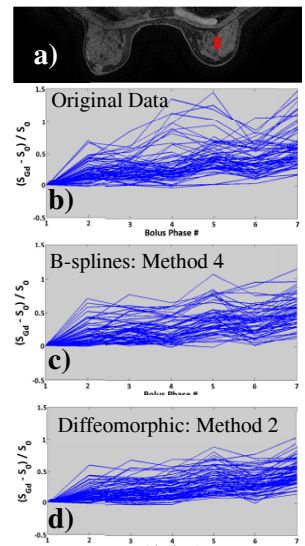


**Figure 2:** Impact of NRR on DCE time courses in a ROI (a). B-splines (b) and diffeomorphic (c) NRR results are compared with original data (d).